

Studying effects of ion exchange resin structure and functional groups on Re(VII) adsorption onto Purolite A170 and Dowex 21K

M.B. Fathi¹, B. Rezaei^{1*}, E.K. Alamdari¹ and R.D. Alorro²

1. Mining and Metallurgical Engineering Department, Amirkabir University of Technology, (Tehran Polytechnic), Tehran, Iran
2. Department of Mining Engineering and Metallurgical Engineering, Western Australian School of Mines, Faculty of Science and Engineering, Curtin University, Kalgoorlie, WA, Australia

Received 28 August 2017; received in revised form 6 October 2017; accepted 10 October 2017
*Corresponding author: rezaei@aut.ac.ir (B. Rezaei).

Abstract

The effects of the functional groups and structures of two different resins, weak base/macroporous and strong base/gel type, Purolite A170 and Dowex 21K on the adsorption properties of Re(VII) ions were investigated experimentally and described by the isotherm, kinetic, and thermodynamic modeling. In this regard, four widely used adsorption isotherm models including Langmuir, Freundlich, Temkin, and Dubinin-Radushkevich (D-R) were subjected to the sorption data in order to describe the reactions involved. Evaluating the correlation coefficients showed that the Freundlich and D-R isotherm models provided the best fit. The Langmuir isotherm capacities (q_m) indicated that the perrhenate ion (ReO_4^-) adsorption was higher for the weak base/macroporous type resin rather than the others (166.67 mg/g and 142.86 mg/g, respectively). Moreover, the results of the EDX studies were in agreement with the previous results. Furthermore, the adsorption kinetics was demonstrated through fitting the data into different mechanisms, among which the pseudo-second-order mechanism was found to be successful for both resins; however, in the case of Dowex 21K, the rate of perrhenate ion uptake was more rapid than that for Purolite A170. Evaluation of the thermodynamic parameters also showed that the reaction mechanism was different for each case and that the adsorption of rhenium on Dowex 21K became more feasible with increase in temperature due to negative values for ΔH .

Keywords: Rhenium, Purolite A170, Dowex 21K, Adsorption Mechanism.

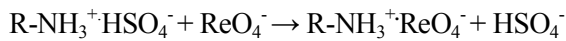
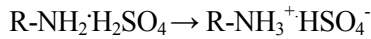
1. Introduction

Rhenium occurs in an scattered form, and since it does not own minerals, it is one of the rarest elements in the Earth's crust with an estimated average concentration of 1 ppb [1]. Since the most stable ionic state of rhenium, 4+, is close to the radii of Mo^{4+} (0.72 Å and 0.70 Å), the common molybdenum ore component is recognized as the main Re-carrier [2]. Moreover, the catalyst spent in the petrochemical industry is the secondary source of rhenium [3].

The unique physical and chemical properties of rhenium such as refractoriness, plasticity, high density, corrosive medium resistance, and catalytic reactivity make it to have more demand in the high-end technologies, i.e. in the metallurgy, and chemical and petrochemical industries. Its wide

industrial applications from one side and its low availability on the other side cause rhenium to be expensive. According to the analyses, the world may face a significant lack of rhenium in the market, so the maximum use of known sources for its production seems to be necessary [4].

At a wide pH range, rhenium is present in solutions, normally as perrhenate anions (ReO_4^-) (Figure 1), and like the other monovalent anions, the perrhenate ions have a strong affinity to anion exchange resins [5]. At low pH values, similar to those in rhenium industrial bear solutions, the reaction of rhenium ion sorption can be accomplished by the direct protonation of resin through the following reactions [6]:



where R-NH₂ represents the matrix of polymer resin and functional group.

It should be mentioned that the single-charged ions ReO₄⁻ having the largest size and thus the lowest capability for hydration, are sorbed on anion exchangers more selectively than the other ions generated by mineral acids [7].

There exist a vast number of investigations on rhenium ion exchange that have examined almost all types of resins. However, there is no systematic data on the rhenium adsorption mechanism based on resin types. In the vast majority of rhenium processing works, the choice of resin has been attributed to the solution composition. Due to the fact that in solutions containing rhenium molybdenum is the main competitor in adsorption on the resin in the case of solutions without molybdenum, the macro-porous resin and the gel-type resin generally have been suggested in solutions containing molybdenum. For the latter, due to its tight structure, it rejects the larger molybdenum molecules (MoO₄²⁻, Mo₇O₂₄⁶⁻, Mo₈O₂₆⁴⁻), while the perrhenate anions can still penetrate the matrix [3].

The whole adsorption process can be detailed based on modeling of the adsorption kinetics, calculating the corresponding equilibrium and

kinetic constants. Knowledge on the adsorption process rate-controlling step including chemical reaction, diffusion or mass transfer can be used to analyze and predict the adsorption rate at any desired conditions that can then be used in designing and modeling the industrial adsorption operations [8]. On the other hand, to optimize the design of an adsorption system for the adsorption of adsorbates, it is of importance to establish the most appropriate isotherm model. Moreover, the adsorbent capacity can be derived by the equilibrium studies. Adsorption equilibria provide the fundamental physico-chemical information to assess the applicability of the adsorption process [9].

Another way for examining a system is thermodynamic studies. The thermodynamic description of the ion-exchange system defines the surface excess as the basic variable describing the separative characteristics of ion exchangers. It determines the boundary conditions for the diffusion process in an ion exchange process. Moreover, the driving force for the diffusion is determinable by thermodynamic science [10].

This work aimed at investigation of the rhenium adsorption behavior by two different functional groups and structures of the Purolite A170 and Dowex 21K resins that are weak base/macroporous and strong base/gel type, respectively.

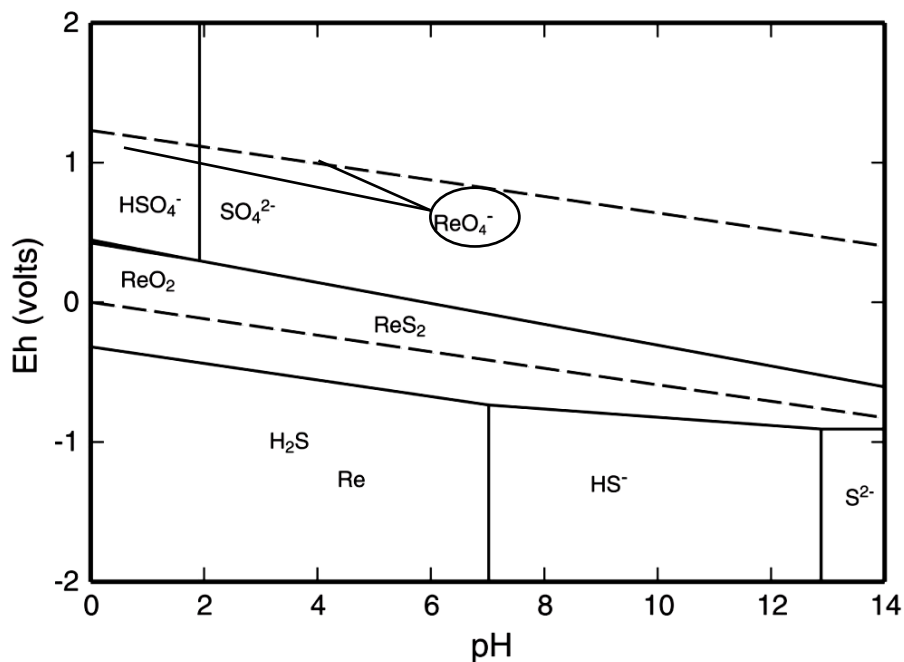


Figure 1. Eh–pH diagram for Re-S-H₂O system (25 °C, 1 bar, ΣS = 10⁻¹, and ΣRe = 10⁻⁶) [36].

2. Theory

2.1. Equilibrium isotherms

The mathematical models that describe the distribution of the adsorbate among the adsorbent and the liquid phase are known as the adsorption isotherms. They are remarkably profitable to explain the possibility of molecules or ions of the adsorbate interaction with sorbent surface sites as well as their degree of accumulation onto the sorbent surface at a constant temperature [11, 12]. Analysis of the equilibrium data obtained using different models is the preliminary step to find out their adequacy to represent the experimental data. In the current work, the most frequently applied isotherm models, namely Langmuir, Freundlich, Temkin, and Dubinin–Radushkevich (Eqs. (1)-(4)) were used to fit the experimental data via the linear regression techniques to demonstrate the phenomena involved in the process of perrhenate ion sorption [11].

$$\text{Langmuir: } \frac{C_e}{q_e} = \frac{C_e}{q_{\max}} + \frac{1}{q_{\max} K_L} \quad (1)$$

$$\text{Freundlich: } \log q_e = \log k_f + \frac{1}{n} \log C_e \quad (2)$$

$$\text{Temkin: } q_e = \frac{RT}{b} \ln A + \frac{RT}{b} \log C_e \quad (3)$$

Dubinin - Radushkevich (D-R):

$$\ln q_e = \ln q_m - \beta \left[RT \ln \left(1 + \frac{1}{C_e} \right) \right]^2, E = \frac{1}{\sqrt{2\beta}} \quad (4)$$

where q_e is the amount of metal adsorbed on resins (mg g^{-1}) in the equilibrium state, C_e is the concentration of the metal remained in the solution (mg L^{-1}), q_{\max} is the maximum loading capacity of the resins used, K_L is the Langmuir constant related to the adsorption energy (L mg^{-1}), K_F is the Freundlich constant related to the adsorption capacity (L mg^{-1}), $1/n$ is the heterogeneity factor, A and b are the Temkin constants, q_m is the Dubinin-Radushkevich monolayer capacity (mg g^{-1}) that is obtained by exponential of y-intercept, β ($\text{mol}^2 \text{kJ}^{-2}$) is a constant with dimensions of energy, and E is the mean free energy of adsorption per mole of the adsorbate (kJ mol^{-1}).

2.2. Kinetic and thermodynamic studies

Analysis of ion exchange kinetics and thermodynamic parameters such as diffusion coefficient, energy and entropy of activation, and free energy change is essential to understand the

mechanism, rate-determining step, rate laws, and ease of the ion exchange process [13]. In the present work, evaluation of the aforementioned parameters was carried out with variation in Re(VII) sorption as a result of temperature change. Modeling of batch kinetic adsorption was performed by the pseudo-first-order, pseudo-second-order, Elovich, and intra-particle diffusion equations. The linear forms of equations can be expressed as follow [11]:

Pseudo-first-order equation:

$$\log(q_e - q_t) = \log q_e - \frac{k_1}{2.303} t \quad (5)$$

Pseudo-second-order equation:

$$\frac{t}{q_t} = \frac{1}{k_2 q_e^2} + \frac{1}{q_e} t \quad (6)$$

$$\text{Elovich equation: } q_t = \frac{1}{\beta} \ln(\alpha\beta) + \frac{1}{\beta} \ln t \quad (7)$$

$$\text{Intra-particle diffusion equation: } q_t = k_i t^{0.5} \quad (8)$$

where, in Eqs. 5 and 6, q_t and q_e are the amount of adsorbate (mg g^{-1}) at any time (t) and at equilibrium, respectively, k_1 is the rate constant of the pseudo-first-order model (h^{-1}), and k_2 ($\text{mg g}^{-1} \text{h}^{-1}$) is the rate constant for the pseudo-second-order model. In Eq. 7, α ($\text{mg g}^{-1} \text{h}^{-1}$) is the initial sorption rate constant, and β (g mg^{-1}) is related to the extent of surface coverage and chemisorptions energy of activation, and in Eq. 8, k_i ($\text{mg g}^{-1} \text{h}^{-0.5}$) is the intra-particle diffusion rate constant.

In order to study the temperature variation impact on the thermodynamic parameters, changes in the Gibbs free energy (ΔG), enthalpy (ΔH), and entropy (ΔS) for the adsorption systems were determined using the following equations:

$$K_{\text{ad}} = \frac{C_a}{C_e} \quad (9)$$

$$\Delta G = -RT \ln K_{\text{ad}} \quad (10)$$

$$\Delta G = \Delta H - T\Delta S \quad (11)$$

$$\ln K_{\text{ad}} = \frac{\Delta S}{R} - \frac{\Delta H}{R} \cdot \frac{1}{T} \quad (12)$$

where R is the gas constant ($8.314 \text{ J}^{-1} \text{ mol}^{-1} \text{ K}^{-1}$), T is the reaction temperature (K), K_{ad} is the adsorption equilibrium constant, and C_a and C_e are the concentrations of Re(VII) on the adsorbent and

solution at equilibrium (mg L⁻¹), respectively. ΔH can be calculated by the slope of the linear Van't Hoff plot (lnK_{ad} versus (1/T) according to Eq. 12) [14].

3. Experimental

3.1. Materials and reagents

The rhenium standard stock solutions were prepared by dissolving NH₄ReO₄ (Aldrich) in doubly distilled water. The ion exchangers Purolite A170 (from Purolite) and Dowex21K (from Dow chemical) (in what follows, A170 and 21K, respectively) were used as the sorbent. The physical and chemical

properties of the resins were tabulated in Table 1. The microstructure of the resins was examined by a Philips XL30 model Scanning Electron Microscopy (SEM). The elemental analysis was conducted using the energy-dispersive X-ray spectroscopy (EDX) DX-series PV 9462/30 (model NEW XL30 144-10). The concentration of metal ions in solutions was determined by Inductively Coupled Plasma-Optical Emission Spectroscopy (ICP-OES, Optima 7300 DV Perkin Elmer). All the reagents used were of analytical grade and used without further purification.

Table 1. Physical and chemical properties of Purolite A170 and Dowex 21K ion exchange resins.

Property	Purolite A170	Dowex 21K
Structure	Macro-porous	gel type
Matrix	Polystyrene/divinylbenzene	Styrene-DVB
Functional group	Complex amine	Quaternary amine
Ionic form	OH (free base)	Cl ⁻
Physical/chemical		
Bead size	0.6–1.2 mm	0.707-0.841mm
Specific gravity	1.05	1.08
Moisture retention	42–47% (in Cl ⁻ form)	50-58% (in Cl ⁻ form)
Total capacity	1.3 meq/mL	1.2 meq/mL

3.2. Experimental procedure

3.2.1. Resin treatment

The A170 anionite preliminary was converted to the SO₄²⁻ form. The weighed amount of resin was kept with 2 mol/L H₂SO₄ for 48 h, and subsequently, led to the swelling of resin. Thereafter, the treated resin was filtered and washed by deionized water till a constant pH value was achieved and later was dried by an oven at 323 ± 1K in a duration of 24 h [15, 16].

The resins A170 and 21K used in the experimental study were subjected to soaking in water overnight before being extracted in aqueous solution for the ReO₄⁻ sorption.

3.2.2. Experimental procedure

The adsorption experiments were carried out under the batch/static conditions using a conical flask (150 mL). The amount of rhenium adsorbed on anionites was determined from the difference between its initial and final concentrations in the solution. All the equilibrium adsorption isotherm experiments were conducted at 288 K. The pH value for the investigated solutions was adjusted to 3 by adding sulfuric acid, and the value was held constant throughout the studied temperature range. 0.1 g of the resins was mixed with 50 mL of the sample solution at different concentrations of [Re⁺⁷]₀ (50mg/L-250 mg/L. The flasks were kept in a thermostated shaker at a speed of 180 rpm for 24 h.

The adsorption kinetics and thermodynamics were investigated by adding 0.1g of the adsorbents to 50 mL solution of 250 mg L⁻¹ of rhenium at different temperatures, e.g. 288, 303, 311, and 321 K. The capacity of the adsorbed metal was calculated using the mass balance equation, as follows:

$$q_c = \frac{C_0 - C_e}{w} v \tag{13}$$

where C₀ is the initial concentration of rhenium in solution (mg/L), C_e stands for the equilibrium concentration measured after adsorption (mg/L); V is the total volume of solution (L), and W is the weight of dry resins (g) [14].

4. Results and discussion

4.1. Studying adsorption isotherms

Adsorption equilibrium tests were carried out at varying levels of the Re concentrations, and the data obtained was plotted based on the parameters of the different models considered (Table 2 and Figures 2 and 3). The calculated relative constants are listed in Table 3. As it can be seen, the experimental data lies well on the isotherm model as the correlation coefficient values (R²) for these plots, and this data is higher than 0.97. The results obtained suggest that all of them can generate a satisfactory fit but both the Freundlich and D-R isotherm models for each adsorbent used show a selectivity coefficient more than 0.99.

Table 2. Initial (C_0) and equilibrium (C_e) concentrations of Re ions in systems with Purolite A170 and Dowex 21K resins.

C_0 (mg/L)	C_e (mg/L) (Purolite A170)	C_e (mg/L) (Dowex 21K)
50	0.224	0.1
100	0.734	0.4
150	1.823	1.2
200	3.453	2.4
250	6.116	4.5

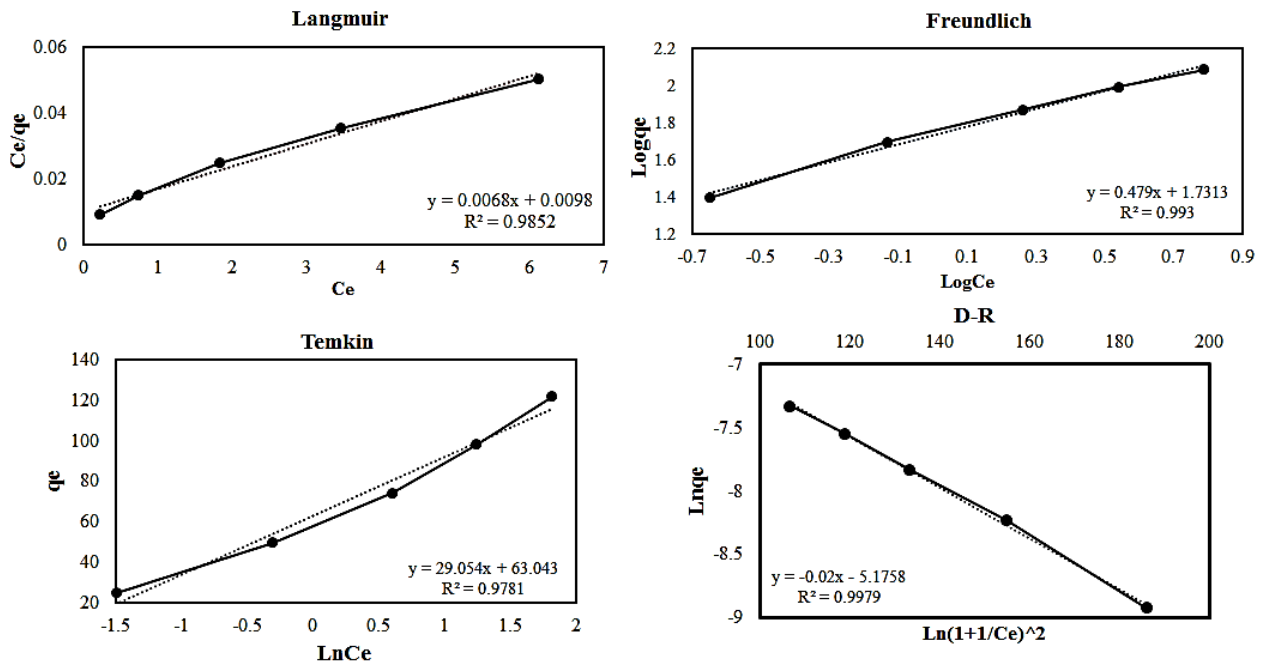


Figure 2. Adsorption isotherms for Re ions by Purolite A170 (pH, 3; contact time, 24 h; temperature, 288 K).

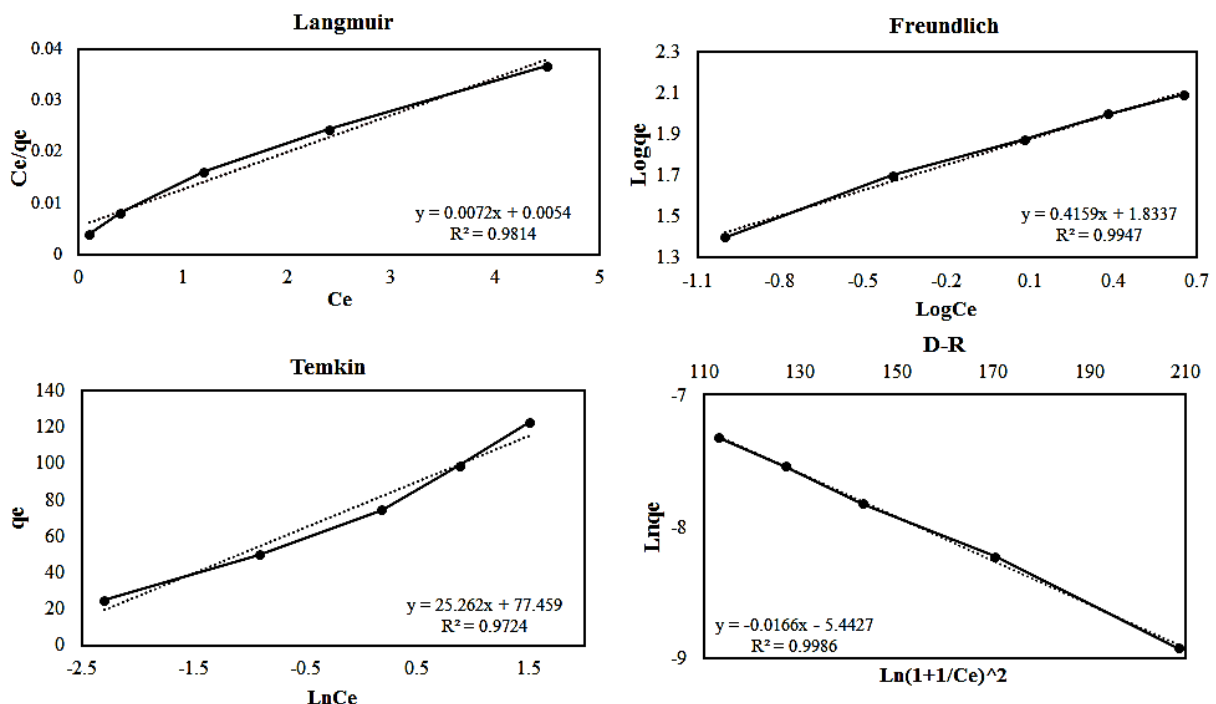


Figure 3. Adsorption isotherms for Re ions by Dowex 21K (pH, 3; contact time, 24 h; temperature, 288 K).

Table 3. Isotherm constants for different models for Re(VII) adsorption on Purolite A170 and Dowex21K.

Resin type	Constants	Purolite A170	Dowex 21K
Langmuir	q_{\max} (mg g ⁻¹)	166.67	142.86
	K_l (L mg ⁻¹)	0.67	1.4
	R^2	0.985	0.981
Freundlich	K_f ((mg/g)/(mg/l) ^{1/n})	53.83	68.08
	n	2.09	2.41
	R^2	0.993	0.994
Temkin	A (L mg ⁻¹)	8.76	21.46
	B (J mg ⁻¹)	83.86	96.44
	R^2	0.978	0.972
Dubinin – Radushkevich (D-R)	q_m (mg g ⁻¹)	0.006	0.004
	B (mol ² k J ⁻²)	3.37*10 ⁻⁹	2.7*10 ⁻⁹
	E (kJ mol ⁻¹)	12.18	13.62
	R^2	0.998	0.998

As shown in Table 3, the maximum monolayer coverage capacities (q_m) from the Langmuir isotherm for A170 and 21K are 166.67 mg/g and 142.86 mg/g, respectively. These results suggest that in the equilibrium state, the operation of the weak base resin with a secondary amine functional group (A170) in rhenium sorption is better than the strong base resins with quaternary amine.

The fit of the data to the Freundlich isotherm shows that the adsorption process is not restricted to one specific class of the sites and assumes heterogeneity of the adsorbent surfaces with different adsorption energies [17, 18]. Researchers have tried to link the Freundlich parameters K_F and $1/n$ to the adsorption mechanisms [19]. Generally, K_F and n are constants incorporating all factors affecting the adsorption capacity and an indication of the favorability of the metal ion adsorption onto the adsorbent, respectively [20]. For classification, as the favorable adsorption value for n should lie in the range of 1-10, a smaller $1/n$ can also be related to a greater adsorption surface heterogeneity. In multi-component systems, a high $1/n$ value indicates a preferential sorption [12]. As seen from the data in Table 3, the n value for both adsorbents is more than one, indicating the favorable and easily adsorption of Re(VII) from the aqueous medium by both resins [17, 21], while the values of $1/n$ for A170 and 21k are 0.478 and 0.415, respectively. The high $1/n$ value for A170 indicates that in competitive situations, perrhenate ions can be adsorbed selectively by this resin [12]. Meanwhile, the low value of $1/n$ for 21k is reflecting the morphology of the gel structure that is more heterogeneous than the A170 adsorption sites.

D-R is another data-adapted model with the best correlation coefficient ($R^2 = 0.998$) for both applied resins. This model is generally used to express the adsorption mechanism [22]. The approach is usually applied to distinguish the

physical and chemical adsorptions of metal ions by a constant E value. The value of E represents the amount of mean free energy required for removing an adsorbate molecule from its location in the sorption space to the infinity [23]. When the value of E is below 8 kJ/mol, the adsorption process can be considered as a physical adsorption. while if it is in the range of 8-16 kJ/mol, it is a chemical adsorption [24, 25]. As summarized in Table 3, in both studied sorbents, the values obtained for mean free energy, E , are above 8 kJ/mol. Therefore, the effect of chemical adsorption plays a dominating role in the adsorption process of ReO_4^- ions on both resins.

4.2. Studying adsorption kinetics and thermodynamic

The kinetic parameters and selectivity coefficient (R^2) were calculated using the presented kinetic models, and the results obtained were summarized in Table 4. It is clear from the R^2 values that for all the studied conditions, the second-order kinetic equation is more applicable than the others for describing the experimental data. Moreover, by comparing the adsorption capacities for the experimental and calculated values, it can be deduced that there are no significant differences between them.

As it can be seen in the results in Table 4, the high value for the pseudo-second-order adsorption rate constant (k_2) for 21K indicates that the uptake of perrhenate ions onto this resin from aqueous solution is more rapid than A170. This is possibly attributed to the presence of the strong base quaternary amine in the functional groups. The rate of uptake can be affected by several factors, e.g. size of adsorbate molecule or ion, adsorbate concentration and its affinity to the adsorbent, diffusion coefficient of the adsorbate in the bulk phase, pore size distribution of the adsorbate, and degree of mixing [14].

Table 4. Kinetic parameters of Re(VII) adsorption onto Purolite A170 (type I) and Dowex 21K (type II).

T (K)	Model	Pseudo-first-order				Pseudo-second-order			Elovich			Intra-particle diffusion	
		Resin type	q_e (exp) (mg g ⁻¹)	q_e (mg g ⁻¹)	K_1 (h ⁻¹)	R^2	q_e (mg g ⁻¹)	K_2 (mg g ⁻¹ h ⁻¹)	R^2	α (mg g ⁻¹ h ⁻¹)	B (g mg ⁻¹)	R^2	K_d (mg g ⁻¹ h ^{0.5})
288	I	116	55.53	0.011	0.992	125	0.00033	0.999	40.83	0.057	0.986	3.07	0.922
	II	124	19.47	0.016	0.815	142.86	0.00132	0.999	7744	0.096	0.724	1.917	0.567
303	I	117	63.62	0.011	0.988	125	0.00034	0.999	43.28	0.057	0.985	3.08	0.92
	II	123.5	6.52	0.013	0.593	125	0.00291	0.999	1051420	0.138	0.664	1.305	0.508
311	I	118	54.76	0.01	0.987	125	0.00036	0.999	56.75	0.06	0.984	2.91	0.917
	II	123	2.94	0.007	0.326	125	0.008	0.999	1.10E+12	0.258	0.52	0.679	0.372
321	I	119	54.32	0.01	0.986	125	0.00037	0.999	63.86	0.062	0.979	2.84	0.907
	II	123	1.28	0.008	0.249	125	0.0049	0.999	3.00E+08	0.187	0.528	0.935	0.378

Identifying the ion exchange process rate limiter and mechanism is commonly performed through using the intra-particle diffusion model [26]. The rate constants for the adsorbents used corresponding to the intra-particle diffusion are shown in Figures 4 and 5; the slope of each portion determines its rate. As it can be seen in Figure 4, there are three stages involved in the adsorption of rhenium on A170 including (1) diffusion of the perrhenate ions from the bulk solution to the film surrounding the adsorbent, (2) their diffusion from the film to the adsorbent surface, and (3) diffusion from the surface to the internal sites [11, 27, 28]. By comparing the slopes, it can be seen that the sharper portion belongs to the adsorbate ions arriving at the adsorbent surrounding film by shaking (180 rpm). However, in Figure 5, it is clear that there are just two steps in the adsorption process on 21K, and the third portion has been omitted, which is most likely to be attributed to the gel structure as well as the small pore diameters (less than 2 nm) of resin compared to the perrhenate ion size that prevent their free penetration and binding of the metal ions onto the inner-active sites of the adsorbent. Thus in this case, despite the presence of the strong base quaternary amine in the functional groups due to the resin gel structure diffusional limitations, the adsorption capacity is reduced. In the selection of an ion exchanger, aside from the type of resin (weak or strong), the internal structure of the resin beads is also an important factor. The beads can either have a porous multi-channelled structure (macro-porous or

macro-reticular resins) or a dense internal structure with no discrete pores (gel resins, also called micro-porous resins). Generally, the macro-porous resins have a high effective surface area such that the ion exchange process is facilitated by providing simple access to the exchange sites for larger ions. On the other hand, in micro-porous resins, solute ions diffuse through the surface of resin particles to interact with the exchanger's inner sites. These resins offer several advantages despite diffusional limitations on the reaction rates, i.e. less fragile, simple handling requirement, faster reaction in functionalization and application reactions, and possessing higher loading capacities [29].

A schematic structure of the macro-porous and gel ion exchangers are shown in Figure 6 [30]. The difference between them lies in their porosity. Using a porogen, macro-pores are introduced into the resins, which ease the access to the active sites and increase the surface area.

To discuss further the influence of resin structure on the Re ion adsorption, the SEM micrographs of the macro-porous and gel resins used were studied in details (Figure 7 (a-d)). As it can be seen in the structures, the surface of macro-porous resin (A170) (Figure 7 (c)) is characterized by the presence of aggregates and pores that facilitate the ion exchange process. In the case of the gel type resin (Figure 7 (d)), the surface has a smooth area with no discrete pores. This decreases the access to the resin's functional groups due to the formation of core particles [31].

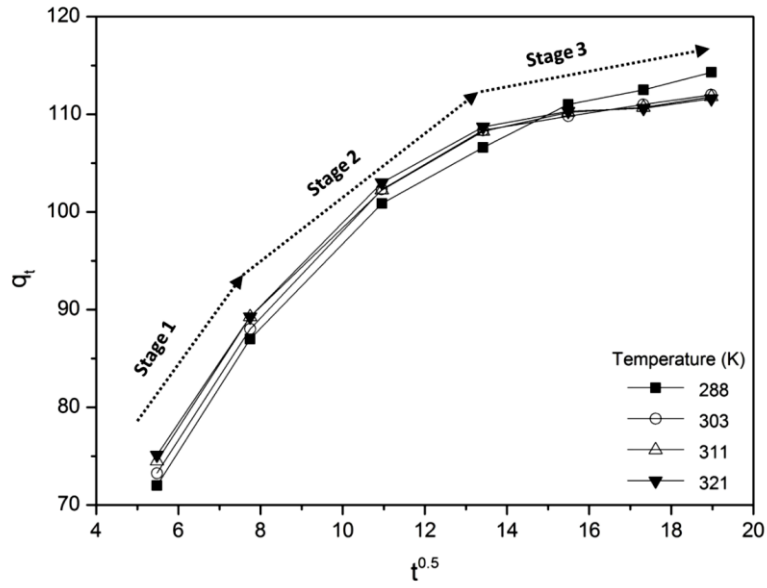


Figure 4. Intra-particle diffusion equation for adsorption of Re(VII) on Purolite A170 resin at different temperatures. Initial concentration of metal ions = 250 mg L⁻¹, resin dosage = 0.1g, pH = 3.

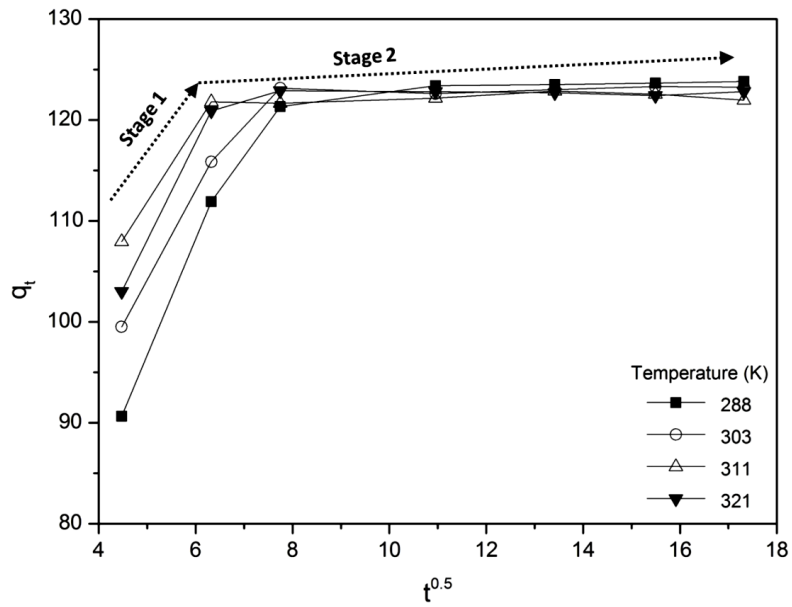


Figure 5. Intra-particle diffusion equation for adsorption of Re(VII) on Dowex 21K resin at different temperatures. Initial concentration of metal ions = 250 mg L⁻¹, resin dosage = 0.1g, pH = 3.

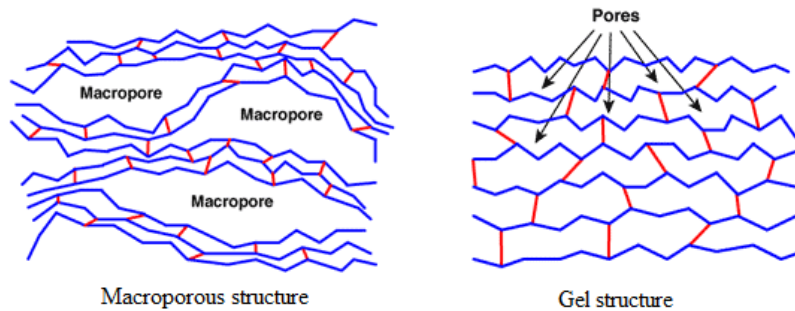


Figure 6. Structure of macro-porous and gel ion exchangers.

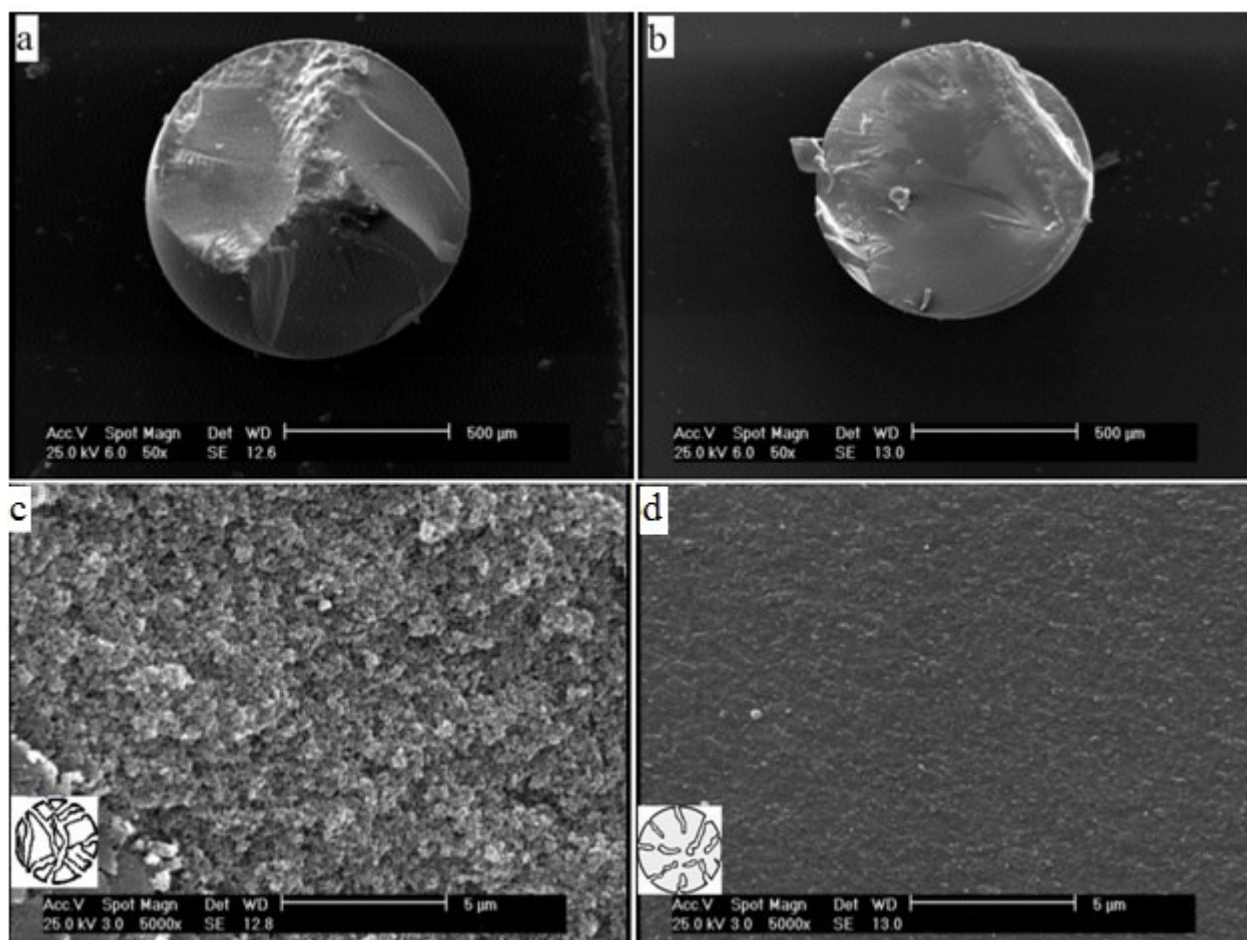


Figure 7. SEM images for Purolite A170: a) overview c) cross-section and Dowex 21K: b) overview d) cross-section.

For an investigate in more details, elemental mapping by SEM-EDX was used for cross-section of the loaded resins. Figures 8 (a) and 8 (b) show the EDX mapping for rhenium. The cross-sectional images show that in the A170 resin (Figure 8a), rhenium is more abundant and has a higher distribution compared to 21K (Figure 8b). These mapping results indicate that Re is able to pass through the resin surface and is concentrated in the inner structure of the macro-porous resin. Generally, comparison of Re distribution in the cross-section surfaces of the studied resins reveals the sieving performance of the gel type resin in perchlorate ion adsorption by inner-active sites rather than the macro type.

As described earlier, the adsorption mechanism can be determined through the thermodynamic quantities such as the change in free energy (ΔG), change in enthalpy of adsorption (ΔH), and change in ΔS . The calculated constants are given in Table 5.

The positive value for ΔH in resin A170 reveals that energy is adsorbed as the ion exchange proceeds, and the reaction is endothermic but in resin 21K, the negative enthalpy value implies two phenomena: (1) the adsorption process is exothermic since in

solution, the hydrated metal ions dissociate into free ions that are then exchanged, and (2) the overcoming of the dehydration energy of rhenium ions during adsorption is exothermic [32].

In Table 5, the variation in ΔG for A170 shows that the values become more negative with increase in temperature, indicating that the sorption process led to a decrease in the Gibbs free energy, confirming the feasibility of the process and spontaneous nature of the process under the current conditions [33].

The ΔS value is an indication of whether the reaction follows an associative or a dissociative mechanism. ΔS values $> -10 \text{ J mol}^{-1} \text{ K}^{-1}$ generally imply a dissociative mechanism, whereas a high negative value or $\Delta S < -10 \text{ J mol}^{-1} \text{ K}^{-1}$ indicates an associative mechanism [13]. The dissociative mechanism can be attributed to the exchange of the metal ions with more mobile ions present on the exchanger, which would cause an increase in the entropy during the adsorption process [34], and also it can be raised from the release of water molecules produced by the ion exchange reaction [35]. In the present work, the positive entropy value for A170 shows the increased randomness at the solid/solution interface during the adsorption process, and it

reconfirms the dissociative mechanism, whereas for other adsorbent, the highly negative ΔS value ($-23.44 \text{ J mol}^{-1} \text{ K}^{-1}$) presents weakening the randomness of the system due to strong bonding between the functional groups on the 21K surface

and perhenate ions as well as the poor accessibility of internal functional groups by perhenate ions for exchange with available mobile ions on them due to the ionite gel structure.

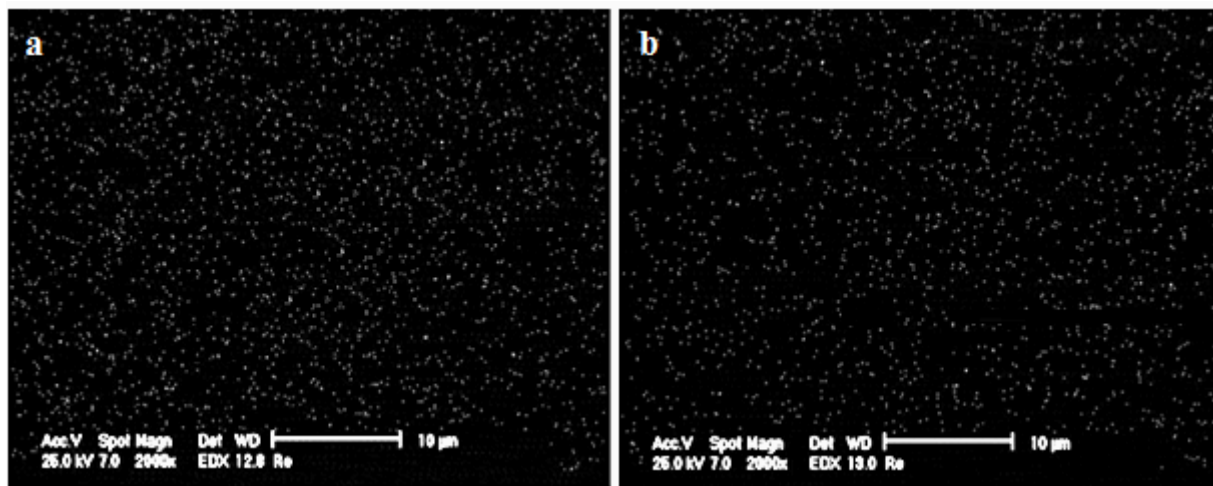


Figure 8. Cross-sectional mapping images of rhenium adsorption by (a) Purolite A170 and (b) Dowex 21K.

Table 5. Thermodynamic parameters of Re(VII) adsorption onto Purolite A170 (type I) and Dowex 21K (type II).

Resin type	ΔH (kJ mol^{-1})	ΔS ($\text{J mol}^{-1} \text{ K}^{-1}$)	ΔG (kJ mol^{-1})			
			T = 288 K	T = 303 K	T = 311 K	T = 321 K
I	3.34	27.31	-4.46	-4.91	-5.14	-5.35
II	-16.56	-23.44	-9.88	-9.36	-9.21	-9.14

5. Conclusions

In this work, alterations of the rhenium ion adsorption behavior by two completely different resins (Purolite A170 and Dowex 21K) were studied. Analysis of the results obtained from four isotherm models showed that adsorption of these ions preferably followed the Freundlich and D-R isotherm models with a selectivity coefficient more than 0.99. Calculation of the saturated maximum adsorption capacity using the Langmuir isotherm showed that despite the presence of the strong base quaternary amine in the functional groups of the 21K resin, due to the gel structure diffusional limitations, the adsorption capacity of this resin was lower than the A170 resin. The results observed from the EDX elemental mapping of cross-sectional loaded resins confirmed the preventive role of the 21K resin gel structure in the adsorption of perhenate ions by inner-vacant sites of ionite. Kinetic studies showed that the adsorption process on both adsorbents followed a pseudo-second-order but in the case of 21K, the rate of perhenate ion uptake was more rapid than the A170 resin. The values for the thermodynamic parameters also suggested that for A170, the adsorption process was spontaneous and endothermic; in addition, the process followed the dissociative mechanism.

However, for 21K, the reaction involved was spontaneous and exothermic; meanwhile, it obeyed an associative mechanism, as revealed by the highly negative entropy values.

Acknowledgments

The authors wish to express their gratitudes to Dr. A. Azadmehr and Engineer M. Torabi for their help and support.

Funding

This work was supported by the National Iranian Copper Industries Co. (NICICO).

References

- [1]. Voudouris, P., Melfos, V., Spry, P.G., Bindi, L., Moritz, R., Ortelli, M. and Kartal, T. (2013). Extremely Re-rich molybdenite from porphyry Cu-Mo-Au prospects in northeastern Greece: Mode of occurrence, causes of enrichment, and implications for gold exploration. *Minerals*. 3 (2): 165-191.
- [2]. da Silva, T. P., Figueiredo, M.O., de Oliveira, D., Veiga, J. P. and Batista, M. J. (2013). Molybdenite as a rhenium carrier: first results of a spectroscopic approach using synchrotron radiation. *Journal of Minerals and Materials Characterization and Engineering*. 1 (05): 207.

- [3]. Van Deventer, J. (2011). Selected ion exchange applications in the hydrometallurgical industry. *Solvent Extraction and Ion Exchange*. 29 (5-6): 695-718.
- [4]. Lipmann, A. (2009). In *Rhenium 2009 and beyond*, Lipmann Walton & Co Ltd.
- [5]. Mikhaylenko, M. and Blokhin, A. (2012). Ion exchange resins tailored for effective recovery and separation of rhenium, molybdenum and tungsten. In Preprint 12–156, SME Annual Meeting, Feb. 19-22, 2012, Seattle, Washington.
- [6]. Dąbrowska, J. and Jermakowicz-Bartkowiak, D. (2008). Modified polymers towards rhenium sorption and desorption. In *Proceedings of the XXIII international symposium on physico-chemical methods of separation*. pp. 6-9.
- [7]. Blokhin, A. A., Amosov, A. A., Murashkin, Y. V., Evdoshenko, S. A., Mikhailenko, M. A. and Nikitin, N.V. (2005). Sorption of rhenium (VII) on gel and macroporous anion exchangers of different basicities from solutions of mineral acids and their ammonium salts. *Russian journal of applied chemistry*. 78 (9): 1411-1415.
- [8]. Fouladgar, M., Beheshti, M. and Sabzyan, H. (2015). Single and binary adsorption of nickel and copper from aqueous solutions by γ -alumina nanoparticles: equilibrium and kinetic modeling. *Journal of Molecular Liquids*. 211: 1060-1073.
- [9]. Senthilkumar, G. and Murugappan, A. (2015), Multicomponent adsorption isotherm studies on removal of multi heavy metal ions in MSW leachate using fly ash. *International Journal of Engineering Research & Technology* (IJERT). V4 (08)
- [10]. R. Araujo, (2004), Thermodynamics of ion exchange, *Journal of non-crystalline solids*, 349 (2004) 230-233.
- [11]. Lou, Z., Zhao, Z., Li, Y., Shan, W., Xiong, Y., Fang, D., Yue, S. and Zang, S. (2013). Contribution of tertiary amino groups to Re (VII) biosorption on modified corn stalk: Competitiveness and regularity. *Bioresource technology*. 133: 546-554.
- [12]. Shahmohammadi-Kalalagh, S. (2011). Isotherm and kinetic studies on adsorption of Pb, Zn and Cu by kaolinite. *Caspian Journal of Environmental Sciences*. 9 (2): 243-255.
- [13]. Khan, M.D.A., Akhtar, A. and Nabi, S.A. (2014). Kinetics and thermodynamics of alkaline earth and heavy metal ion exchange under particle diffusion controlled phenomenon using polyaniline-sn (iv) iodophosphate nanocomposite. *Journal of Chemical & Engineering Data*. 59 (8): 2677-2685.
- [14]. Xiong, Y., Xu, J., Shan, W., Lou, Z., Fang, D., Zang, S. and Han, G. (2013). A new approach for rhenium (VII) recovery by using modified brown algae *Laminaria japonica* adsorbent. *Bioresource technology*. 127: 464-472.
- [15]. Abisheva, Z.S. and Zagorodnyaya, A.N. (2011). Rhenium of kazakhstan (review of technologies for rhenium recovery from mineral raw materials in kazakhstan). In book of proceedings. p. 208.
- [16]. Joo, S.H., Kim, Y.U., Kang, J.G., Kumar, J.R., Yoon, H.S. and Shin, S.M. (2012). Recovery of rhenium and molybdenum from molybdenite roasting dust leaching solution by ion exchange resins. *Materials transactions*. 53 (11): 2034-2037.
- [17]. Xiong, C. and Yao, C. (2010). Adsorption behavior of MWAR toward Gd (III) in aqueous solution. *Iranian Journal of Chemistry and Chemical Engineering (IJCCE)*. 29 (2): 59-66.
- [18]. Nur, T., Loganathan, P., Nguyen, T. C., Vigneswaran, S., Singh, G. and Kandasamy, J. (2014). Batch and column adsorption and desorption of fluoride using hydrous ferric oxide: Solution chemistry and modeling. *Chemical Engineering Journal*. 247: 93-102.
- [19]. Sparks, D. L. (2003). *Environmental soil chemistry*. Academic press.
- [20]. Kadirvelu, K., Goel, J. and Rajagopal, C. (2008). Sorption of lead, mercury and cadmium ions in multi-component system using carbon aerogel as adsorbent. *Journal of Hazardous Materials*. 153 (1): 502-507.
- [21]. Xiong, C., Yao, C. and Wu, X. (2008). Adsorption of rhenium (VII) on 4-amino-1, 2, 4-triazole resin. *Hydrometallurgy*. 90 (2): 221-226.
- [22]. Günay, A., Arslankaya, E. and Tosun, I. (2007). Lead removal from aqueous solution by natural and pretreated clinoptilolite: adsorption equilibrium and kinetics. *Journal of Hazardous Materials*. 146 (1): 362-371.
- [23]. Gupta, A.K. and Ayoob, S. (2016). *Fluoride in Drinking Water: Status, Issues, and Solutions*. CRC Press.
- [24]. Liu, J., & Wang, X. (2013). Novel silica-based hybrid adsorbents: lead (II) adsorption isotherms. *The Scientific World Journal*. <http://dx.doi.org/10.1155/2013/897159>
- [25]. Singha, B. and Das, S.K. (2013). Adsorptive removal of Cu (II) from aqueous solution and industrial effluent using natural/agricultural wastes. *Colloids and Surfaces B: Biointerfaces*. 107: 97-106.
- [26]. Wu, F.C., Tseng, R.L. and Juang, R. S. (2009). Initial behavior of intraparticle diffusion model used in the description of adsorption kinetics. *Chemical Engineering Journal*. 153 (1): 1-8.
- [27]. Igwe, J. and Abia, A.A. (2006). A bioseparation process for removing heavy metals from waste water using biosorbents. *African journal of biotechnology*. 5 (11).
- [28]. Qiu, H., Lv, L., Pan, B. C., Zhang, Q. J., Zhang, W. M. and Zhang, Q. X. (2009). Critical review in adsorption

kinetic models. Journal of Zhejiang University-Science A. 10 (5): 716-724.

[29]. Mal'tseva, E.E., Blokhin, A.A. and Murashkin, Y.V. (2012). Specific features of rhenium desorption from weakly basic anion exchangers Purolite A170 and Purolite A172 with ammonia solutions. Russian Journal of Applied Chemistry. 85 (7): 1034-1040.

[30]. Hubicki, Z. and Kołodyńska, D. (2012). Selective removal of heavy metal ions from waters and waste waters using ion exchange methods. In Ion Exchange Technologies. InTech.

[31]. Coutinho, F.M.B., Carvalho, D.L., Aponte, M.L.T. and Barbosa, C.C.R. (2001). Pellicular ion exchange resins based on divinylbenzene and 2-vinylpyridine. Polymer. 42 (1): 43-48.

[32]. Liu, W., Zhang, P., Borthwick, A.G., Chen, H. and Ni, J. (2014). Adsorption mechanisms of thallium (I) and thallium (III) by titanate nanotubes: Ion-exchange and co-precipitation. Journal of colloid and interface science. 423: 67-75.

[33]. Xiong, C. (2008). Sorption behaviour of D 155 resin for Ce (III). Indian journal of chemistry. Section A, Inorganic, bio-inorganic, physical, theoretical & analytical chemistry. 47: 1377-1380.

[34]. Xiong, C., Chen, X. and Liu, X. (2012). Synthesis, characterization and application of ethylenediamine functionalized chelating resin for copper preconcentration in tea samples. Chemical engineering journal. 203: 115-122.

[35]. Lee, I.H., Kuan, Y.C. and Chern, J.M. (2007). Equilibrium and kinetics of heavy metal ion exchange. Journal of the Chinese Institute of Chemical Engineers. 38 (1): 71-84.

[36]. Nebeker, N. and Hiskey, J.B. (2012). Recovery of rhenium from copper leach solution by ion exchange. Hydrometallurgy. 125: 64-68.

مطالعه تأثیر ساختار و گروه‌های عاملی دو رزین تبادل یونی پرولایت A170 و داوکس 21K بر روی جذب یون‌های Re(VII)

محمد باقر فتحی^۱، بهرام رضایی^{۱*}، اسکندر کشاورز علمداری^۱ و ریچارد دیاز آلورو^۲

۱- دانشکده مهندسی معدن و متالورژی، دانشگاه صنعتی امیرکبیر، ایران

۲- دانشکده مهندسی معدن و متالورژی، دانشگاه کرتین، استرالیا

ارسال ۲۰۱۷/۸/۲۸، پذیرش ۲۰۱۷/۱۰/۱۰

* نویسنده مسئول مکاتبات: rezai@aut.ac.ir

چکیده:

در این تحقیق تأثیر نوع ساختار و نوع گروه‌های عاملی دو رزین مختلف، بازی ضعیف/متخلخل و بازی قوی/غیر متخلخل، پرولایت A170 و داوکس 21K بر روی رفتار جذب یون‌های Re(VII) به طور آزمایشگاهی مورد بررسی قرار گرفت و نتایج توسط مدل‌های ایزوترم، سینتیک و ترمودینامیک تشریح شدند. در این راستا، چهار مدل ایزوترم شامل لانگموور، فرنلیچ، تمکین و دوینین-رادشکوچ به منظور تعیین مکانیسم فرآیند به کار گرفته شد. محاسبه ضرایب برازش نشان داد که برای هر دو رزین، مدل‌های فرنلیچ و دوینین-رادشکوچ تطابق مناسب‌تری با داده‌های آزمایشگاهی دارند. در چنین شرایطی ماکزیم ظرفیت جذب محاسبه شده از مدل لانگموور برای یون‌های مذکور مشخص کرد که این پارامتر برای رزین بازی ضعیف بیشتر از نوع بازی قوی است (۱۶۶/۶۷mg/g و ۱۴۲/۸۶mg/g)، که این نتایج توسط مطالعه مقاطع رزین‌های باردار به وسیله روش EDX مورد تأیید قرار گرفت. تحلیل داده‌های سینتیکی توسط مکانیسم‌های مختلف نشان داد که مدل شبه مرتبه دوم برای هر دو رزین بهترین برازش را داشته و همچنین رزین داوکس 21K سرعت جذب خیلی بالایی نسبت به رزین پرولایت A170 دارا است. با محاسبه و ارزیابی پارامترهای ترمودینامیکی مشخص شد که مکانیسم جذب برای هر رزین متفاوت بوده و همچنین به علت منفی بودن علامت ΔH ، با افزایش دما فرآیند جذب یون‌های رنیوم بر روی رزین داوکس 21K بهتر و راحت‌تر انجام می‌پذیرد.

کلمات کلیدی: رنیوم، پرولایت A170، داوکس 21K، مکانیسم جذب.